

Study of the $pd(dp) \rightarrow {}^3\text{He} \pi\pi$ reactions close to threshold

F. Bellemann,¹ A. Berg,¹ J. Bisplinghoff,¹ G. Bohlscheid,¹ J. Ernst,¹ C. Henrich,¹ F. Hinterberger,¹
 R. Ibal,¹ R. Jahn,^{1,*} R. Joosten,¹ K. Kilian,² A. Kozela,³ H. Machner,⁴ A. Magiera,⁵ J. Munkel,¹
 P. von Neumann-Cosel,⁶ P. von Rossen,² H. Schnitker,¹ K. Scho,¹ J. Smyrski,⁵ R. Tölle,² and C. Wilkin⁷

(The COSY-MOMO collaboration)

¹*Institut für Strahlen- und Kernphysik, Universität Bonn, D-53115 Bonn, Germany*

²*Institut für Kernphysik, Forschungszentrum Jülich, D-52425 Jülich, Germany*

³*Institute of Nuclear Physics, PL-31342 Kraków, Poland*

⁴*Fakultät für Physik, Universität Duisburg-Essen, Lotharstrasse 1, D-47048 Duisburg, Germany*

⁵*Institute of Physics, Jagellonian University, PL-30059 Kraków, Poland*

⁶*Institut für Kernphysik, Technische Universität Darmstadt, D-64289 Darmstadt, Germany*

⁷*Physics and Astronomy Department, UCL, London WC1E 6BT, United Kingdom*

(Dated: September 12, 2018)

New experimental data on the $pd \rightarrow {}^3\text{He} \pi^+ \pi^-$ reaction obtained with the COSY-MOMO detector below the three-pion threshold are presented. The reaction was also studied in inverse kinematics with a deuteron beam and the higher counting rates achieved were especially important at low excess energies. The comparison of these data with inclusive $pd \rightarrow {}^3\text{He} X^0$ rates allowed estimates also to be made of $\pi^0 \pi^0$ production. The results confirm our earlier findings that close to threshold there is no enhancement at low excitation energies in the $\pi^+ \pi^-$ system, where the data seem largely suppressed compared to phase space. Possible explanations for this behavior, such as strong p waves in the $\pi^+ \pi^-$ system or the influence of two-step processes, are explored.

PACS numbers: 13.75.Cs, 25.10.+s, 25.40.Qa

I. INTRODUCTION

The ABC effect is an enhancement of the two-pion invariant mass ($M_{\pi\pi}$) spectrum close to threshold that has been observed in certain nuclear reactions. It manifests itself through a peak at a mass of about 310 MeV/ c^2 with a width ≈ 50 MeV/ c^2 . However, these values change with experimental conditions and there is much evidence to show that the ABC is a kinematic effect, associated with the presence of nucleons, rather than being a genuine s -wave $\pi\pi$ resonance [1].

The effect was first identified by Abashian, Booth, and Crowe (ABC) in measurements of the inclusive cross sections for $pd \rightarrow {}^3\text{He} X^0$ at a beam energy of $T_p = 743$ MeV [2]. The lack of a similar signal in the $pd \rightarrow {}^3\text{H} X^+$ case shows that the effect has to be dominantly in the $\pi\pi$ isospin $I_{\pi\pi} = 0$ channel. Apart from phase space effects, one would then expect that the $\pi^+ \pi^-$ component in the production of the ABC should be twice as strong as the $\pi^0 \pi^0$.

The original ABC data covered only production of the ${}^3\text{He}$ in the forward hemisphere with respect to the proton beam direction in the center-of-mass system (CMS) [2]. By using a deuteron beam with an energy about twice as high, the acceptance was increased significantly and

allowed the ABC effect to be observed inclusively in both hemispheres at Saclay [3].

In order to discuss data in different kinematic regions, it is convenient to label them in terms of the excess energy $Q = W - M_{{}^3\text{He}} - 2M_\pi$, where W is the total CMS energy. The original inclusive ABC data were obtained at $Q = 184$ MeV with respect to the charged pion threshold [2]. Exclusive measurements of both the $pd \rightarrow {}^3\text{He} \pi^+ \pi^-$ and $pd \rightarrow {}^3\text{He} \pi^0 \pi^0$ differential cross sections were carried out at the even higher excess energy of $Q = 269$ MeV by the CELSIUS-WASA collaboration [4] and these were complemented by later measurements of $pd \rightarrow {}^3\text{He} \pi^0 \pi^0$ at $Q = 338$ MeV by the WASA collaboration at COSY [5, 6]. The data supported the conclusion that at low $\pi\pi$ invariant mass $M_{\pi\pi}$ the ABC effect was of dominantly isoscalar ($I_{\pi\pi} = 0$) nature, though corrections had to be made to account for the pion mass differences. However, the charged pion data suggested that there could be some $I_{\pi\pi} = 1$ contribution at large $M_{\pi\pi}$. When the kinematics of the full three-body final state were reconstructed, the exclusive experiments also allowed the distributions in the $\pi^3\text{He}$ invariant mass to be evaluated. These seemed to show some reflections of the $\Delta(1232)$ distribution.

Although the systematics were less well controlled, much higher statistics on the $dp \rightarrow {}^3\text{He} \pi^+ \pi^-$ reaction at a similar excess energy were obtained by the COSY-ANKE collaboration by using a deuteron beam incident on a hydrogen target [7]. The difference between the $\pi^+ {}^3\text{He}$ and $\pi^- {}^3\text{He}$ invariant mass distributions was an

*E-mail: jahn@hiskp.uni-bonn.de

indication of some interference between $I_{\pi\pi} = 1$ and $I_{\pi\pi} = 0$ amplitudes. It should be noted that, although the set-ups of the CELSIUS-WASA and ANKE experiments were very different, both sets of measurements were carried out in the forward CM hemisphere between the incident proton and final ${}^3\text{He}$.

Both the WASA and the ANKE experiment show the importance of the $\Delta(1232)$ in two-pion production at high excess energies and so it is not unexpected that the results could look rather different at low Q , *i.e.*, below the threshold for Δ production. Nevertheless, there was surprise when the first exclusive $pd \rightarrow {}^3\text{He}\pi^+\pi^-$ results emerged from the COSY-MOMO collaboration; these showed that at $Q = 70$ MeV there was no sign of any ABC effect [8]. The data were low compared to phase space at small $M_{\pi\pi}$ and, indeed, they could be modeled as if there were a p -wave between the $\pi^+\pi^-$ pair. No comparison of the $\pi^+{}^3\text{He}$ and $\pi^-{}^3\text{He}$ invariant mass distributions could be made because, in the absence of a magnetic field in the MOMO detector, it was not possible to distinguish the sign of the charge on an individual pion. However, the absence of an ABC effect even closer to threshold was confirmed in low-statistics data obtained at $Q = 28$ MeV at CELSIUS [9]. The different behavior between low and high Q was also noted in the quasi-free production reaction $dd \rightarrow n_{\text{sp}}{}^3\text{He}\pi^0\pi^0$, where n_{sp} is a *spectator* neutron that was reconstructed from the measurements of the ${}^3\text{He}$ and two neutral pions in the WASA detector [5, 6]. The Fermi motion in the deuteron allowed the authors to estimate the cross section for $pd \rightarrow {}^3\text{He}\pi^0\pi^0$ over a range of values of Q .

In view of the marked differences between the observations for large and small excess energy, it was decided to carry out further measurements with the MOMO detector at excess energies above and below our previous value of $Q = 70$ MeV. The experimental set-up, with the ${}^3\text{He}$ being measured in a high resolution spectrograph and the charged pions the MOMO detector, is described in some detail in Sec. II. One conclusion that is evident from this discussion is that the acceptance for the $dp \rightarrow {}^3\text{He}\pi^+\pi^-$ reaction with a deuteron beam is significantly higher than that with incident protons. The doubling of the incident momenta leads to generally faster particles that are pushed into smaller angular regions. The gain by using a deuteron beam is especially important at low excess energy Q because the cross section falls very rapidly as threshold is approached.

Data taken in pd kinematics are first presented at an excess energy of $Q = 92$ MeV to investigate the anti-ABC effect first noted in the MOMO 70 MeV results [8]. Estimates of the cross sections for $pd \rightarrow {}^3\text{He}\pi^0\pi^0$ were also made in both these cases by comparing the data sets obtained with and without the $\pi^+\pi^-$ detection in MOMO. The comparison of charged and neutral pion data indicates that there must be a very significant fraction of $I_{\pi\pi} = 1$ production at these energies. This is consistent with the direct measurements of the $pd \rightarrow {}^3\text{He}\pi^+\pi^-$ and $pd \rightarrow {}^3\text{He}\pi^0\pi^0$ cross sections carried out at CELSIUS at

$Q = 28$ MeV [9]. This energy was repeated with higher statistics at MOMO in pd kinematics [10] before being investigated fully with a deuteron beam. The consistency of the MOMO pd and dp data at $Q \approx 28$ MeV gives confidence in the acceptance estimates in the analysis. This allowed data to be taken with a deuteron beam at $Q = 8$ MeV, which would have been highly problematic in pd kinematics. The results of these measurements are reported in Sec. III.

Though a suppression of the data at low $M_{\pi\pi}$ might be a signal for p -wave pion pairs, there are other possibilities, as discussed in Sec. IV. In a two-step model the reaction is closely linked to that for $\pi^-p \rightarrow \pi^0\pi^0n$ [11], where the sum of a contact term and production via the Roper resonance can also deplete the cross section near the $\pi\pi$ threshold [12]. Our conclusions and suggestions for further work are presented in Sec. V.

II. EXPERIMENTAL SET-UP

The layout of the experimental setup with the MOMO (Monitor Of Mesonic Observables) detector was described in our previous publication that reported the $pd \rightarrow {}^3\text{He}K^+K^-$ measurements [13]. An external proton or deuteron beam from the COSY accelerator of the Forschungszentrum Jülich was incident on a 4 mm thick liquid deuterium or hydrogen target with 1.5 μm mylar windows [14]. A beam diameter of less than 2 mm led to precise determination of the emission angles.

The ${}^3\text{He}$ ions produced close to threshold in the $dp(pd) \rightarrow {}^3\text{He}\pi\pi$ reaction are confined to a small cone around the beam direction and these were analyzed with the high resolution spectrograph Big Karl [15]. Particle tracks were measured in the focal plane by two planes of multi-wire drift chambers (MWDC), six chambers in each plane, followed by two planes of scintillator walls. These walls allow particle identification via $\Delta E - E$ as well as time-of-flight (TOF) measurements. As is seen from Fig. 1, this combination led to the ${}^3\text{He}$ being well separated from tritons and deuterons even without requiring pion detection in MOMO. The measurement of just the ${}^3\text{He}$ yields the inclusive cross section for $dp(pd) \rightarrow {}^3\text{He}X$ reaction so that such data would be comparable to those obtained in the initial ABC experiments [2, 3]. However, because the present experiments were carried out at low excess energy, the unobserved state X must correspond to $\pi^+\pi^-$ or $\pi^0\pi^0$.

In order to reconstruct more completely the $pd(dp) \rightarrow {}^3\text{He}\pi^+\pi^-$ events, the Big Karl spectrograph was supplemented by the MOMO detector, which measured the two charged pions [13]. MOMO consists of 672 scintillating fibers, arranged in three planes, denoted by (1,2,3) in Fig. 2. The fibers are individually read out by 16-anode multichannel photomultipliers. The fibers in the three planes are rotated by 60° with respect to each other and hits in three layers are required in order to avoid combinatorial ambiguities. It is important to note that the sign

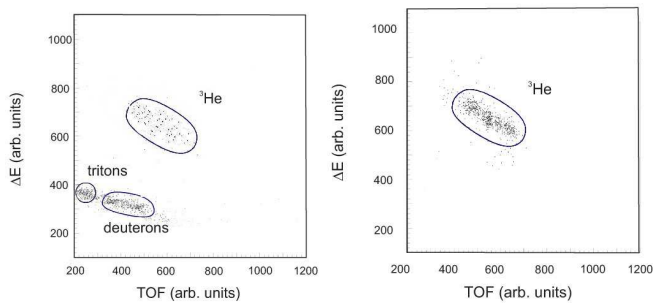


FIG. 1: Left panel: Particle identification in the focal plane of Big Karl for proton-deuteron collisions at an excess energy of $Q = 70$ MeV with respect to the ${}^3\text{He}\pi^+\pi^-$ threshold. Events are plotted as function of the energy loss in the first scintillator wall ΔE and the time of flight (TOF) between the scintillator walls. The dominant proton events are suppressed by imposing a threshold in the ΔE measurement. Right panel: Same as Left but with the additional requirement of two hits in the MOMO detector. This eliminates almost completely the triton and deuteron events and confirms well the position and extent of the ${}^3\text{He}$ band.

of the charge on each of the pions is not determined and this automatically leads to the symmetrization of some of the differential distributions.

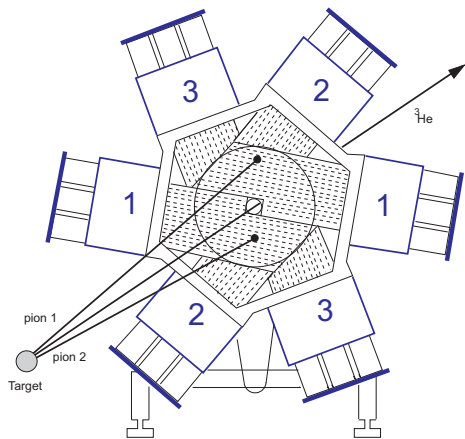


FIG. 2: (Color online) Front view of the MOMO vertex detector with the indication of a typical event. Both the primary beam and the recoil ${}^3\text{He}$ detected in Big Karl pass through the central hole. The numbers denote the different layers and the three boxes at the end of each read-out symbolize the phototubes.

The MOMO detector was placed perpendicular to the beam direction 20 cm downstream of the target, outside a vacuum chamber, the end wall of which was a 5 mm thick aluminum plate. The detector and its location are illustrated in Fig. 3. The central hole, which subtended an angle of 6° at the target, allowed the passage of the primary beam and also the ${}^3\text{He}$ that were detected in Big Karl. The maximum angle of 45° was set by the physical

dimensions of MOMO.

Each of the scintillating fibers is 2.5 mm thick but, when operating with a deuteron beam, these were too thin to provide reliable energy information. The MOMO wall was therefore complemented by a hodoscope consisting of 16 wedge-shaped 2 cm thick scintillators. This hodoscope, which is also shown in Fig. 3, was already used in the study of the $pd \rightarrow {}^3\text{He}K^+K^-$ reaction [13].

The luminosity required to deduce absolute cross sections was measured in two different ways. In the first method, applied in all runs, the luminosity was measured with calibrated monitor counters placed in the forward hemisphere, left and right of the target. During the calibration of the monitors, the number of scattered particles was compared with the intensity of the direct beam, as measured with scintillators in the beam exit of Big Karl. To avoid dead-time effects in the hodoscope, the beam intensity was reduced by de-bunching the beam between the ion source and the cyclotron injector. For sufficiently small beam intensity the relation between monitors and hodoscope is linear. In the actual production runs the counting rates in the monitors was small enough to reduce the dead-time effects to a negligible level. The systematic uncertainty in the beam intensity obtained using this procedure is estimated to be 5%. Combining this with a target thickness uncertainty, that is also about 5%, the total systematic uncertainty in the cross section normalization is conservatively estimated to be below 10%.

The results were controlled by a second method that is independent of the target thickness. Elastic pd or dp scattering was studied with two telescopes that measured protons and deuterons in coincidence. The telescopes, each consisting of two silicon counters, were placed left and right of the target at positions determined by elastic scattering kinematics. The normalization was then deduced using the cross sections for elastic proton-deuteron scattering taken from the compilation of Ref. [16]. The results of the two methods were consistent within error bars.

Although, unlike the CELSIUS experiments [4, 9], there was no π^0 detector, it was still possible to extract estimates for the $pd(dp) \rightarrow {}^3\text{He}\pi^0\pi^0$ cross section by comparing the inclusive $pd(dp) \rightarrow {}^3\text{He}X^0$ cross section deduced from the Big Karl measurement with that for $pd(dp) \rightarrow {}^3\text{He}\pi^+\pi^-$ obtained from the combined Big Karl and MOMO data. However, such a subtraction does depend on precise evaluations of the $\pi^+\pi^-$ acceptance in MOMO.

The acceptance of the overall system for the measurement of the ${}^3\text{He}\pi^+\pi^-$ final state is generally much higher for the deuteron than the proton beam. Part of this is due to the tighter forward cone of the ${}^3\text{He}$ detected in Big Karl but there other important effects of the forward momentum boost, in particular the higher probability that the pions will emerge with angles below 45° and thus be detected in MOMO. Decay losses are also less in inverse kinematics. The overall acceptance estimates for the standard and inverse kinematics are presented in

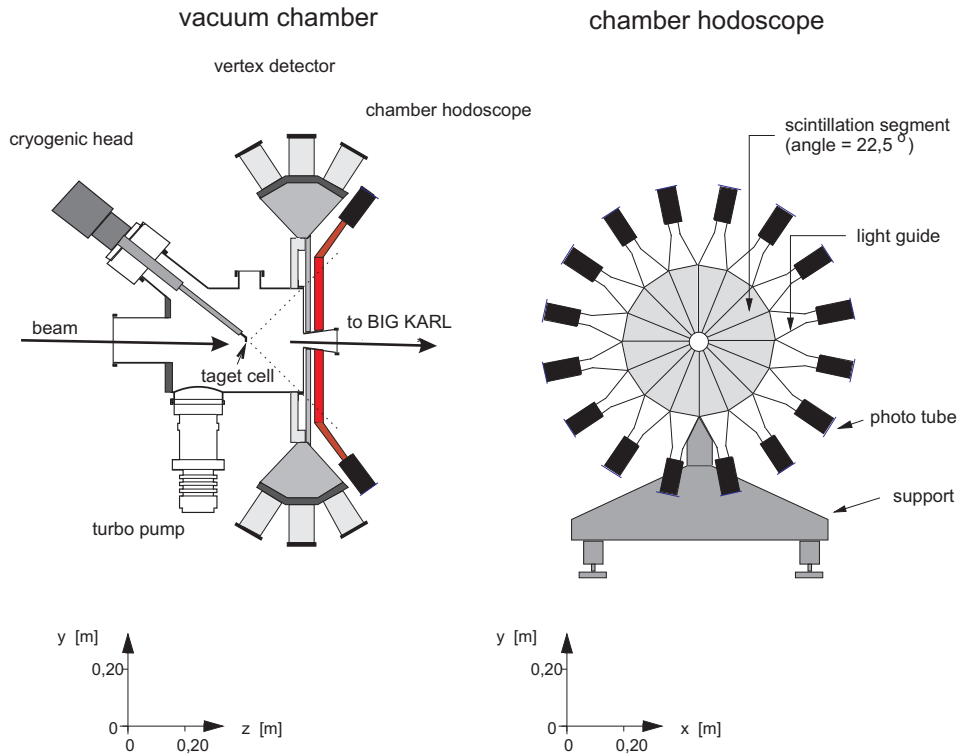


FIG. 3: (Color online) Left panel: Cross section through the target area showing the location of the MOMO vertex hodoscope. The final wall in beam direction is the segmented scintillator hodoscope (shown in red). Right panel: View onto the segmented hodoscope placed after the MOMO detector.

Fig. 4 for the energy ranges relevant for the current measurements.

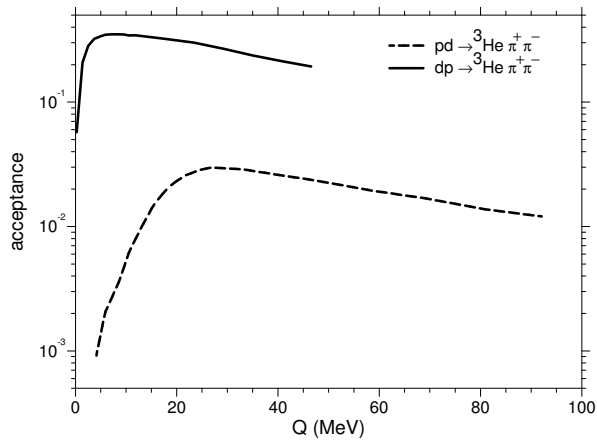


FIG. 4: Comparison of the acceptances of the full detection system for the $pd \rightarrow {}^3\text{He} \pi^+ \pi^-$ and $dp \rightarrow {}^3\text{He} \pi^+ \pi^-$ reactions as functions of the excess energy Q .

The acceptance falls at very low Q because of the beam-pipe hole shown in Fig. 3 but, away from this region, it decreases steadily with increasing Q , though with the acceptance in inverse kinematics being about an order of magnitude higher than with the proton beam. This

factor is not compensated by the differences in beam intensities, which were typically 5×10^8 protons per spill of 4 s length and 11 s repetition rate and 7×10^9 deuterons per spill of 30 s length. Measurements with the proton beam are therefore severely limited for both low and high excess energy.

III. EXPERIMENTAL RESULTS

The previous MOMO measurement of $pd \rightarrow {}^3\text{He} \pi^+ \pi^-$ at $Q = 70$ MeV [8] is shown in Fig. 5(a) along with analogous data obtained at $Q = 92$ MeV in Fig. 5(b). The message from the two data sets is similar; there is no sign of any ABC enhancement and the shapes of the differential cross sections look much closer to phase space weighted by the $\pi\pi$ excitation energy than pure phase space.

By comparing the inclusive data obtained just with the use of Big Karl with those where there was also signals in the MOMO detector it was possible to get the estimates of the $pd \rightarrow {}^3\text{He} \pi^0 \pi^0$ cross section at $Q = 79$ MeV and $Q = 101$ MeV shown in Figs. 5(c) and (d), respectively. The higher excess energies noted here are a consequence of the pion mass differences. These data are typically an order of magnitude lower than for charged pion production. This indicates that, although $I_{\pi\pi} = 0$ production is

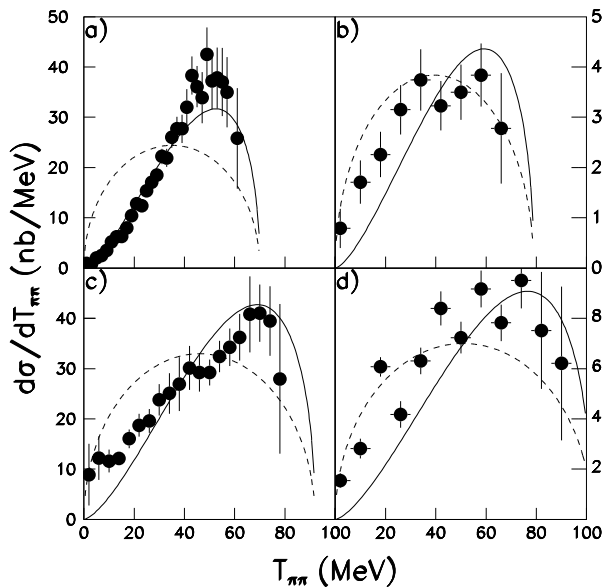


FIG. 5: MOMO measurements of the differential cross section for $pd \rightarrow {}^3\text{He} \pi^+ \pi^-$ at a) $Q = 70$ MeV and c) $Q = 92$ MeV and $pd \rightarrow {}^3\text{He} \pi^0 \pi^0$ at b) $Q = 79$ MeV and d) $Q = 101$ MeV as functions of the excitation energy $T_{\pi\pi}$ in the $\pi\pi$ system. The dashed curves are non-relativistic phase-space distributions normalized to the integrated cross sections and the solid ones represent phase space multiplied by a $T_{\pi\pi}$ factor and similarly normalized.

not negligible at these energies, the dominant production must be in $I_{\pi\pi} = 1$. The non-vanishing of the isovector production was already evident in the direct measurements at CELSIUS at $Q = 28$ MeV [9].

Given that the $\pi^0\pi^0$ data were obtained by comparing two big numbers, the associated error bars are much larger and it is less easy to make firm conclusions regarding the shapes of the distributions. Nevertheless, there does seem to be some tendency for the cross sections to be pushed to higher $\pi\pi$ excitation energies than would be suggested by phase space.

Data on the $pd \rightarrow {}^3\text{He} \pi^+ \pi^-$ reaction had been obtained at CELSIUS at $Q \approx 28$ MeV [9]. In view of the limited statistics in the CELSIUS experiment, we have used the MOMO detector to explore this region with both proton and deuteron beams. All three data sets are shown in Fig. 6 where, in order to compare the shapes of the distributions, the CELSIUS results have been reduced by a factor of 0.5. This factor is significant in comparison to the quoted 10% statistical uncertainty in the luminosity [9].

The shapes of the three data sets are broadly consistent. Any difference between the MOMO pd and dp normalizations is not inconsistent with the overall systematic uncertainties discussed earlier. However, it must be noted that in pd kinematics there is a loss of acceptance for very large $\pi^+ \pi^-$ excitation energies and no points are

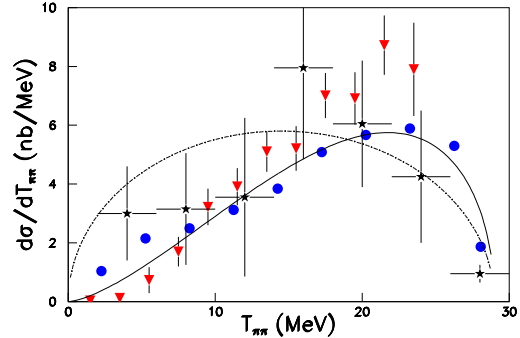


FIG. 6: (Color online) Cross section for the production of the ${}^3\text{He} \pi^+ \pi^-$ final state at an excess energy of $Q \approx 28$ MeV as a function of the excess energy $T_{\pi\pi}$ in the $\pi\pi$ rest frame. The (blue) circles are MOMO data taken with a deuteron beam whereas the (red) inverted triangles are the corresponding proton beam data [10]. The CELSIUS data [9] have been reduced by a factor of 0.5 before being shown by the (black) stars. The chain curve is an arbitrarily normalised phase space distribution and the solid curve is that weighted with a $T_{\pi\pi}$ factor.

shown above about 24 MeV.

There is little sign of an ABC effect, *i.e.*, any enhancement at low $\pi\pi$ excitation energy $T_{\pi\pi}$, though the larger acceptance dp data do show more strength in this region than the pd results. Just as for the original 70 MeV MOMO data, the results are better described by weighting the phase space distribution by a $T_{\pi\pi}$ factor, as if the two pions were emerging in a relative p wave.

The distortion of phase space is far less evident in the distribution in the $\pi^3\text{He}$ energies shown in Fig. 7. Unlike the higher energy data [4, 7], the lack of a magnetic field did not allow separate plots to be made for π^+ and π^- .

There are no major discrepancies between the two MOMO data sets at $Q = 28$ MeV, which is some confirmation of the reliability of the MOMO acceptance evaluations. Nevertheless, it must be assumed that the results obtained with the deuteron beam are the more reliable because of the much larger acceptance shown in Fig. 4.

Exactly the same behavior is seen at $Q = 8$ MeV as that commented upon at 28 MeV. Thus the $\pi^+ \pi^-$ distribution shown in Fig. 8a is well described if the phase-space function is modified by a $T_{\pi\pi}$ factor. On the other hand, the $\pi^3\text{He}$ distribution of Fig. 8b shows much less deviation from phase space though this may, in part, be linked to this being an average of the $\pi^+ {}^3\text{He}$ and $\pi^- {}^3\text{He}$ spectra.

The clearest proof for the importance of higher partial waves in the $dp \rightarrow {}^3\text{He} \pi^+ \pi^-$ reaction even as close to threshold as $Q = 28$ MeV is provided by the distribution in the Gottfried-Jackson angle θ_{GJ} [18]. This is the angle between the relative momentum between the two pions

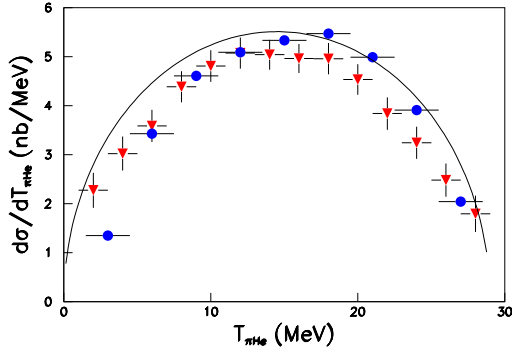


FIG. 7: (Color online) Cross section for the $dp \rightarrow {}^3\text{He}\pi^+\pi^-$ (blue circles) and $pd \rightarrow {}^3\text{He}\pi^+\pi^-$ (red inverted triangles) reactions at an excess energy of $Q \approx 28$ MeV as a function of the excess energy $T_{\pi^3\text{He}}$ in the $\pi^3\text{He}$ rest frame. These MOMO data are compared with an arbitrarily normalized non-relativistic phase space distribution.

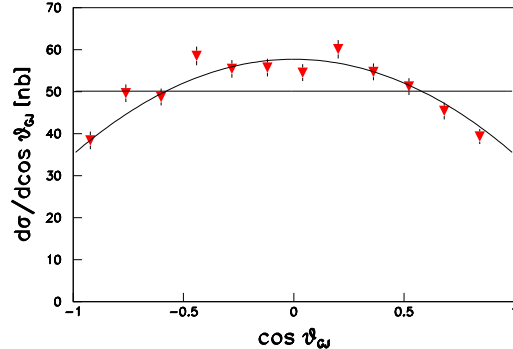


FIG. 9: (Color online) Distribution of the MOMO $dp \rightarrow {}^3\text{He}\pi^+\pi^-$ data at $Q = 28$ MeV in the Gottfried-Jackson angle. The data are symmetric about 90° because the sign of the charges on the pions was not measured. The curve shown, $d\sigma/d\cos\theta_{GJ} = 57.7 - 22.6\cos^2\theta_{GJ}$, is a best fit to the data assuming a linear dependence in $\cos^2\theta_{GJ}$.

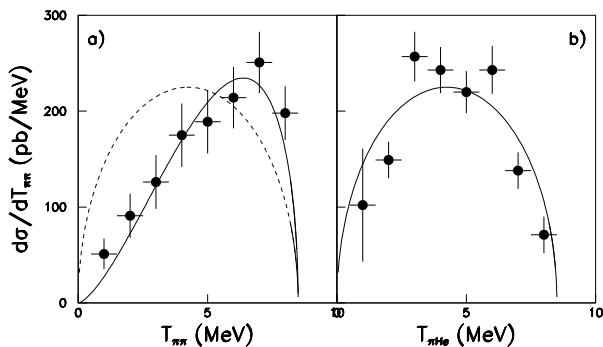


FIG. 8: MOMO measurements of the differential cross section for the $dp \rightarrow {}^3\text{He}\pi^+\pi^-$ reaction at $Q = 8$ MeV in terms of a) the excitation energy in the $\pi^+\pi^-$ system, and b) in the $\pi^3\text{He}$ system. The dashed curve in a) shows the shape of the phase-space distribution whereas the solid one is phase space modified by a $T_{\pi\pi}$ factor. In the $\pi^3\text{He}$ system of b), only the phase-space shape is shown.

and the direction of the deuteron beam, evaluated in the dipion rest frame. Any anisotropy here is a signal for higher partial waves in the $\pi^+\pi^-$ system. The MOMO data shown in Fig. 9 are symmetric about 90° because the π^+ and π^- are not distinguished in this detector. The clear deviation from isotropy proves that the dipion cannot be in a pure s wave. Such a behavior could be a signal for a superposition of s - and p -wave pion pairs but higher partial waves are not definitively excluded. The sign of the $\cos^2\theta_{GJ}$ term is opposite to that we found for K^+K^- production [13], though this could be influenced

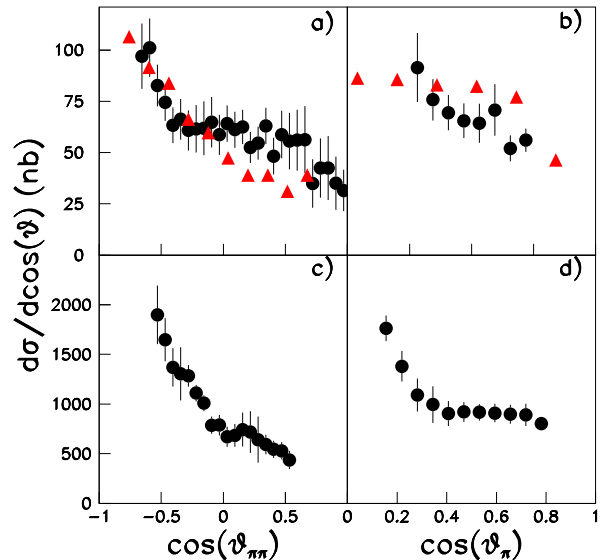


FIG. 10: (Color online) Differential cross section for the $dp \rightarrow {}^3\text{He}\pi^+\pi^-$ at excess energies of $Q = 28$ MeV (a+b) and $Q = 92$ MeV (c+d) in terms of the pion opening angle $\theta_{\pi\pi}$ and the angle θ_π between the outgoing pion and the incoming beam direction, both angles being evaluated in the overall c.m. frame. The (black) circles were taken in pd kinematics but at $Q = 28$ MeV data (blue triangles) were also obtained in dp kinematics with a much enhanced acceptance.

by ϕ production.

Other angular distributions can be derived from the MOMO data and we show in Fig. 10 those with respect

to the $\pi^+\pi^-$ opening angle, $\theta_{\pi\pi}$, and one pion with respect to the beam direction, θ_π , both in the overall CM frame. At $Q = 28$ MeV data were obtained in both the original pd kinematics and also with the much increased acceptance offered by dp kinematics. The biggest disagreement between the 28 MeV results obtained with the two kinematics is at large $\cos\theta_{\pi\pi}$ in Fig. 10a. This is the region preferentially associated with small $T_{\pi\pi}$ and we already saw a similar discrepancy in Fig. 6.

Further evidence for the anomalous behavior of the $pd(dp) \rightarrow {}^3\text{He}\pi\pi$ reaction at low energies is to be found in the variation of the total cross section with Q that is shown in Fig. 11. A simple Q^2 phase-space dependence describes well the $pd(dp) \rightarrow {}^3\text{He}\pi^0\pi^0$ data but near threshold the Q^3 dependence seen for $pd(dp) \rightarrow {}^3\text{He}\pi^+\pi^-$ must reflect the presence of higher partial waves. However, at $Q \approx 270$ MeV, where the ABC enhancement is obvious [4], the Q^3 dependence must have moderated considerably. This suggests that there might be some $I_{\pi\pi} = 1$ contribution that is important at low Q that becomes less significant at high Q . This conclusion is consistent with the CELSIUS isospin decomposition at low energy [9].

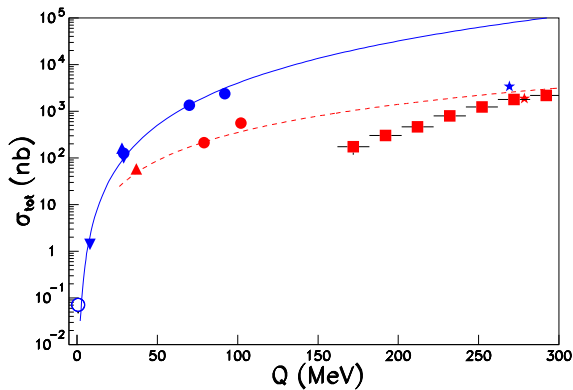


FIG. 11: (Color online) Dependence of the total cross sections for $pd(dp) \rightarrow {}^3\text{He}\pi^+\pi^-$ (blue) and $pd(dp) \rightarrow {}^3\text{He}\pi^0\pi^0$ (red) on the excess energy Q . The curves are arbitrarily normalized Q^3 and Q^2 shapes for $\pi^+\pi^-$ and $\pi^0\pi^0$ production, respectively. The closed circles represent MOMO pd data whereas those taken in dp are shown as inverted triangles. The triangles are low energy CELSIUS points [9] and the stars are high energy CELSIUS-WASA points obtained in pd kinematics [4], renormalized by a factor of 1.5 [6]. The squares represent $pd \rightarrow {}^3\text{He}\pi^0\pi^0$ data obtained in dd collisions within a spectator model [5, 6]. The near-threshold UCF measurement [17] is indicated by an open circle. It should be noted that the data points cannot be distinguished for $Q \approx 28$ MeV.

Values of the $pd \rightarrow {}^3\text{He}\pi^0\pi^0$ total cross section were also obtained from measurements of the $dd \rightarrow n_{\text{sp}} {}^3\text{He}\pi^0\pi^0$ reaction, assuming that the unobserved neutron to be a true *spectator*. By measuring the ${}^3\text{He}$ and

the two π^0 , the reaction could be studied over a wide Q range while using a fixed deuteron beam energy of 1.7 GeV [5, 6]. The energy dependence indicated by these points shown in Fig. 11 seems to be at odds with the data at lower Q but it must be stressed that this conclusion does depend on the use of the spectator model for large Fermi momenta.

IV. INTERPRETATION

There is no universally accepted model for the ABC effect in the $pd \rightarrow {}^3\text{He}X^0$ reaction but it is clear from all the data shown in Sec. III that the possible presence of an ABC effect depends strongly upon the excess energy. Below $Q \approx 100$ MeV there is no sign of any ABC enhancement.

It has been argued that the ABC effect is closely associated with the decay of the $d^*(2380)$ dibaryon resonance in $np \rightarrow d\pi^0\pi^0$ [19] and that this resonance might also play an important role in more complicated reactions, such as $pd \rightarrow {}^3\text{He}X^0$ [20]. Although this does offer a natural explanation for the strong energy dependence of the ABC production, the momentum transfers seem to be very large for a model involving a $d^*(2380)$ and a spectator nucleon.

There is good evidence that at high Q the ABC effect is dominantly isoscalar in character. On the other hand, at $Q = 28$ MeV the production of isovector pion pairs is the larger and, at our two highest energies, isoscalar production, though small, is certainly non-zero. As a consequence the $\pi^+\pi^-$ pair cannot be purely in a relative p -wave with $I_{\pi\pi} = 1$, as we assumed earlier when describing our $Q = 70$ MeV data [8].

Nevertheless, the $\pi^+\pi^-$ data for $Q < 100$ MeV could still be described in terms of a dominant p -wave plus a small amount of s -wave that is required by the $\pi^0\pi^0$ data of Fig. 5. This would still yield an energy dependence of the total cross section that is close to the Q^3 fit shown in Fig. 11. One difficulty with this assumption is to be found in the shapes of the $\pi^0\pi^0$ spectra shown in Figs. 5b and 5d. Though the uncertainties here are large, due to the subtraction of the $\pi^+\pi^-$ data from the inclusive spectra, they seem to show features that are similar to the $\pi^+\pi^-$ distributions, with a preference to higher $T_{\pi\pi}$ values than those suggested by phase space. This is what might be expected in a two-step model [11].

A classical two-step model was first proposed for η production in the $pd \rightarrow {}^3\text{He}\eta$ reaction [21] and this was later put on a quantum mechanical basis [22]. When applied to two-pion production, it is assumed that the reaction consists of pion production through $pp \rightarrow d\pi^+$ followed by $\pi^+n \rightarrow \pi^+\pi^-(\pi^0\pi^0)p$, with the final proton and deuteron fusing to form the observed ${}^3\text{He}$ [11]. As currently implemented, only the contribution from isoscalar pion pairs has been estimated as a function of the excitation energy in the $\pi\pi$ system. The predictions of the model for the differential distributions at the highest MOMO en-

ergy are compared with the experimental data in Fig. 12, where the normalization of the form factors is determined from the threshold rate of the $pd \rightarrow {}^3\text{He} \eta$ reaction [22].

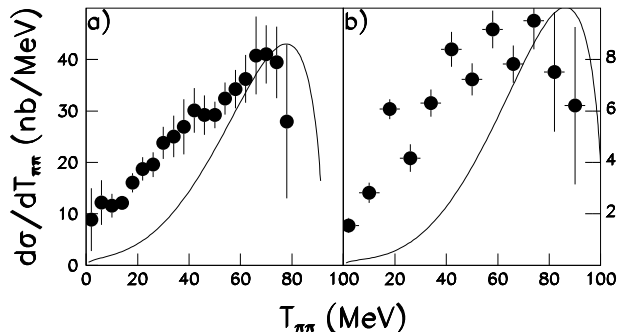


FIG. 12: a) Differential cross section for $pd \rightarrow {}^3\text{He} \pi^+ \pi^-$ at $Q = 92$ MeV compared to the predictions of the two-step model [11]. b) Differential cross section for $pd \rightarrow {}^3\text{He} \pi^0 \pi^0$ at $Q = 101$ MeV obtained by comparing data with and without signals in the MOMO detector. The theoretical predictions for $\pi^0 \pi^0$ production are reduced by a factor of 0.3.

The curves are both pushed towards the maximum $T_{\pi\pi}$ but, since this corresponds to isoscalar pion pairs, it is not due to pion p waves but it is rather a feature of the $\pi^+ n \rightarrow \pi^+ \pi^- (\pi^0 \pi^0) p$ amplitude, which was taken from the Valencia model [12]. This striking behavior is due to a cancellation at low $\pi\pi$ excitation energies between a contact term and the contribution from the Roper resonance. The model was tuned to fit the $\pi^- p \rightarrow \pi^0 \pi^0 n$ experimental data in the low Q region and it is not valid to continue it to higher energies to investigate the ABC phenomenon. Despite its failings at low $T_{\pi\pi}$, the model predicts the right order of magnitude for $\pi^+ \pi^-$ production, though the predictions have to be reduced by a factor of 0.3 in order to describe the $\pi^0 \pi^0$ data.

The predictions of the energy dependence of the total cross sections for isoscalar pion pair production in the $pd \rightarrow {}^3\text{He} \pi^+ \pi^-$ and $pd \rightarrow {}^3\text{He} \pi^0 \pi^0$ reactions are shown in Fig. 13. Given the uncertainty in the model and the fact that only the $I_{\pi\pi} = 0$ contribution is predicted, the estimate of the $pd \rightarrow {}^3\text{He} \pi^+ \pi^-$ total cross section is reasonable. The same cannot be said for the $pd \rightarrow {}^3\text{He} \pi^0 \pi^0$ prediction. Though it is close to the value obtained by the CELSIUS group at 37 MeV [9], the curve is over three times too high compared to the MOMO data at 79 and 101 MeV. The MOMO values, of course, result from indirect measurements, so that systematic uncertainties may be large.

The only way that a factor of ten between the $\pi^+ \pi^-$ and $\pi^0 \pi^0$ production cross sections could arise is if the $I_{\pi\pi} = 1$ production were very much stronger than $I_{\pi\pi} = 0$. If this proves to be the case, the two-step model must have given a gross overestimate of the $I_{\pi\pi} = 0$ contribution to $\pi^+ \pi^-$ production.

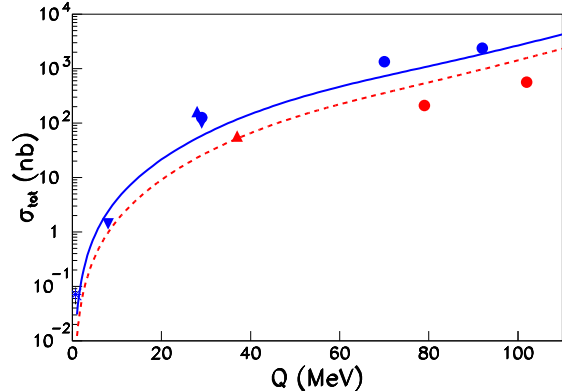


FIG. 13: (Color online) The low energy data of Fig. 11, showing total cross sections for the $pd \rightarrow {}^3\text{He} \pi^+ \pi^-$ and $pd \rightarrow {}^3\text{He} \pi^0 \pi^0$ reactions. These are compared with the predictions of the two-step model of Ref. [11] for isoscalar $\pi\pi$ pairs. The solid (blue) curve is for $\pi^+ \pi^-$ production and the dashed (red) curve for $\pi^0 \pi^0$.

V. CONCLUSIONS

New data have been presented on both the $pd \rightarrow {}^3\text{He} \pi^+ \pi^-$ and $dp \rightarrow {}^3\text{He} \pi^+ \pi^-$ reactions at excess energies $Q < 100$ MeV, where the ${}^3\text{He}$ was measured in a high resolution spectrograph and the charged pions in the MOMO vertex detector. Though the results obtained are generally consistent, the acceptance of the whole system is much higher with the deuteron beam and these results are much to be preferred. In all cases the differential cross sections seemed suppressed at low $M_{\pi\pi}$ invariant masses compared to phase space and there was certainly no sign in the $\pi^+ \pi^-$ spectrum of the ABC enhancement that is so prevalent in higher energy data.

Though, as we previously reported [8], the data could be an indication of isovector $\pi^+ \pi^- p$ -waves, there are other possible explanations and the behavior could be governed by that present in the $\pi^- p \rightarrow \pi^0 \pi^0 n$ amplitudes, where p -waves are forbidden. Such a model does reproduce features of the observed mass distributions but it would have to be extended to include both $I_{\pi\pi} = 1$ contributions and angular distributions before it could be considered a satisfactory theory. Of particular importance in this regard is the distribution in the Gottfried-Jackson angle, where our data clearly prove that there must be contributions from higher partial waves in the $\pi\pi$ system at energies even as low as $Q = 28$ MeV.

The comparison of data taken with and without a charged pion signal in MOMO allowed estimates to be made for the $pd \rightarrow {}^3\text{He} \pi^0 \pi^0$ production rates. The systematic uncertainties are, of course, larger and direct measurements, such as those achieved with WASA [4],

should also be attempted. The comparison of the current MOMO $\pi^+\pi^-$ and $\pi^0\pi^0$ data for $Q > 70$ MeV can only be understood if the pion pairs are overwhelmingly produced with $I_{\pi\pi} = 1$.

For $Q \gtrsim 180$ MeV there is a strong ABC effect whereas for $Q \lesssim 100$ MeV the ABC is completely absent. Data are sadly lacking in the intermediate energy interval to show how the ABC develops between 100 and 180 MeV. The only quality data that exist in this region were taken in deuteron-deuteron collisions [5, 6] and they rely on the spectator model being valid at large Fermi momenta. The situation can only be clarified by measurements of free $dp \rightarrow {}^3\text{He}\pi^+\pi^-$ and $dp \rightarrow {}^3\text{He}\pi^0\pi^0$ reactions in this energy range.

ACKNOWLEDGEMENTS

We wish to thank the COSY machine crew for providing the high quality proton and deuteron beams necessary for these experiments. We are also indebted to the Big Karl technical staff for their tireless efforts. Correspondence with Dr Perez del Rio, who provided the numerical values of the quasi-free data used in Fig. 11, has been most helpful. Support by Forschungszentrum Jülich (FFE) and Bundesministerium für Bildung und Forschung (BMBF) is gratefully acknowledged.

-
- [1] C. Amsler *et al.* in J. Beringer *et al.* (Particle Data Group), Phys. Rev. D **86**, 010001 (2012).
 - [2] A. Abashian, N. E. Booth, and K. M. Crowe, Phys. Rev. Lett. **5**, 258 (1960); A. Abashian *et al.*, Phys. Rev. **132**, 2296 (1963).
 - [3] J. Banaigs *et al.*, Nucl. Phys. B **67**, 1 (1973).
 - [4] M. Bashkanov *et al.*, Phys. Lett. B **637**, 223 (2006).
 - [5] P. Adlarson *et al.*, Phys. Rev. C **91**, 015201 (2015).
 - [6] E. Perez del Rio, PhD thesis, University of Tübingen (2014); <http://hdl.handle.net/10900/53837>.
 - [7] M. Mielke *et al.*, Eur. Phys. J. A **50**, 102 (2014).
 - [8] F. Belleman *et al.*, Phys. Rev. C **60**, 061002 (1999).
 - [9] M. Andersson *et al.*, Phys. Lett. B **485**, 327 (2000).
 - [10] G. Bohlscheid, PhD thesis, University of Bonn (1998).
 - [11] G. Fäldt, A. Gårdestig, and C. Wilkin, Phys. Lett. B **496**, 185 (2000).
 - [12] M. J. Vicente Vacas and E. Oset, Phys. Rev. C **60**, 064621 (1999).
 - [13] F. Belleman *et al.*, Phys. Rev. C **75**, 015204 (2007).
 - [14] V. Jaeckle *et al.*, Nucl. Instrum. Meth. A **349**, 15 (1994).
 - [15] M. Drochner *et al.*, Nucl. Phys. A **643**, 55 (1998).
 - [16] S. Steltenkamp, Master thesis, Westfälische Wilhelms-Universität Münster (2002).
 - [17] A. C. Betker *et al.*, Phys. Rev. Lett. **77**, 3510 (1996).
 - [18] K. Gottfried and J. D. Jackson, Nuovo Cimento **33**, 309 (1964).
 - [19] M. Bashkanov *et al.*, Phys. Rev. Lett. **102**, 052301 (2009).
 - [20] P. Adlarson *et al.*, Phys. Rev. C **86**, 032201(R) (2012).
 - [21] K. Kilian and H. Nann, AIP Conf. Proc. **221**, 185 (1991).
 - [22] G. Fäldt and C. Wilkin, Nucl. Phys. A **587**, 769 (1995).